BIOCHEMISTRY
including biophysical chemistry & molecular biology

Article

pubs.acs.org/biochemistry

The Elevated Copper Binding Strength of Amyloid-β Aggregates Allows the Sequestration of Copper from Albumin: A Pathway to Accumulation of Copper in Senile Plaques

Dianlu Jiang,[†] Lin Zhang,[†] Gian Paola G. Grant,[†] Christopher G. Dudzik,[‡] Shu Chen,[†] Sveti Patel,[†] Yuanqiang Hao,[†] Glenn L. Millhauser,[‡] and Feimeng Zhou*,[†]

[†]Department of Chemistry and Biochemistry, California State University, Los Angeles, Los Angeles, California 90032, United States
[‡]Department of Chemistry and Biochemistry, University of California, Santa Cruz, Santa Cruz, California 95064, United States

Supporting Information

ABSTRACT: Copper coexists with amyloid-β (Aβ) peptides at a high concentration in the senile plaques of Alzheimer's disease (AD) patients and has been linked to oxidative damage associated with AD pathology. However, the origin of copper and the driving force behind its accumulation are unknown. We designed a sensitive fluorescent probe, Aβ(1−16)(Y10W), by substituting the tyrosine residue at position 10 in the hydrophilic domain of Aβ(1−42) with tryptophan. Upon mixing Cu(II), Aβ(1−16)(Y10W), and aliquots of Aβ(1−42) taken from samples incubated for different lengths of time, we found that the Cu(II) binding strength of aggregated Aβ(1−42) has been elevated by more than 2 orders of magnitude with respect to that of monomeric Aβ(1−42). Electron paramagnetic spectroscopic measurements revealed that the Aβ(1−42) aggregates, unlike their monomeric form, can seize copper from human serum albumin, an abundant copper-containing protein in brain and cerebrospinal fluid. The significantly elevated binding strength of the Aβ(1−42) aggregates can be rationalized by a Cu(II) coordination sphere constituted by three histidines from two adjacent Aβ(1−42) molecules. Our work demonstrates that the copper binding affinity of Aβ(1−42) is dependent on its aggregation state and provides new insight into how and why senile plaques accumulate copper in vivo.

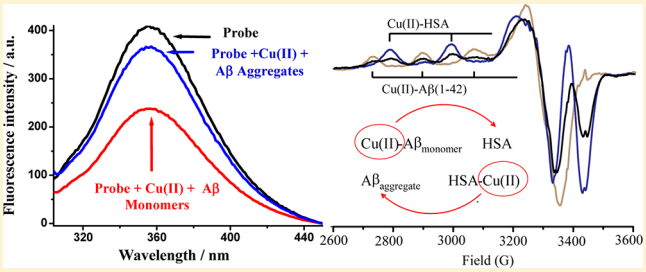

Senile plaques, comprising mainly amyloid β (Aβ) peptides[1,2] and constituting one of the pathological hallmarks of Alzheimer's disease (AD), accumulate abnormally high concentrations of metals [e.g., Cu(II) at ∼0.4 mM and Fe(III) at ∼0.9 mM][3] in AD-afflicted brains. Efforts to understand the interaction between metals and Aβ have been made to correlate the presence and amounts of metals to AD pathogenesis.[4,5] In particular, copper has received a considerable amount of attention in the field, because of its involvement in redox cycling to produce reactive oxygen species (ROS) and to exert possible oxidative damage in AD.[4−13] A Raman spectral analysis of post-mortem tissues from AD brains revealed that methionine residues of Aβ peptides are oxidized and the oxidation was attributed to ROS facilitated by copper redox cycling.[14] Nevertheless, the origin and driving force behind the accumulation of copper in senile plaques have remained entirely unclear. At odds is the fact that monomeric Aβ peptides bind copper with a moderate affinity constant (10^9−10^{10} M^{-1}; or a nanomolar dissociation constant K_d).[15−18] Such a binding strength is not sufficiently high for Aβ monomers to sequester copper from copper-transporting proteins.[19,20] Human serum albumin (HSA) is the major copper chelator and transporter protein in blood plasma,[19,20] with a K_a value of ∼10^{12} M^{-1} or a dissociation constant K_d value in the picomolar range.[21,22] It is also the major protein in the cerebrospinal fluid (CSF) that is known to be in contact with senile plaques.[23] Although HSA is a viable source of copper, a recent study by Faller and co-workers showed that in vitro copper bound by monomeric Aβ can be readily removed by HSA.[24] Thus, the Aβ monomer is clearly not responsible for the accumulation of copper in senile plaques. The K_d value of monomeric Aβ(1−42) was measured by Serell et al. to be 60 pM,[18] which is substantially (1−5 orders of magnitude) lower than values determined by other studies (cf. Table S1 of the Supporting Information for a comprehensive list of the K_d values reported in the literature). Even such a binding strength was considered to be insufficient for seizing copper from HSA.[18]

The high abundance of Aβ fibrils in senile plaques suggests the possibility that Aβ aggregates might possess a higher strength in binding copper and consequently be involved in the sequestration and enrichment of copper in senile plaques. The finding that senile plaques can be dissolved by strong copper chelators implies that copper helps stabilize Aβ aggregates.[25]

Received: August 3, 2012
Revised: December 12, 2012
Published: December 13, 2012

Thus far, there is a lack of direct evidence showing the aggregation-dependent enhancement of the copper binding strength of Aβ. It is worth noting that zinc, another metal that accumulates in senile plaques, appears to bind to Aβ aggregates at a slightly higher (approximately 2-fold) affinity than to the Aβ monomers.[26,27]

Here we report the use of a nonaggregating, copper-binding Aβ mutant, Aβ(1−16)(Y10W) (Table 1), as a fluorescent probe to monitor the elevated copper binding strength of aggregated Aβ. The intrinsic Tyr residue at position 10 of Aβ(1−42) has been widely used for fluorescence measurements of the copper binding constants of various Aβ peptides (cf. Table S1 of the Supporting Information and references cited therein). As shown in this work, substitution of Tyr-10 of Aβ(1−16) with a Trp residue affords a much higher fluorescence quantum yield and a wavelength different from that of native Aβ(1−42). Furthermore, unlike Aβ(1−42), such a probe does not aggregate and become insoluble when complexed with Cu(II). Consequently, in a competitive binding assay, the use of a soluble probe with a similar Cu(II) binding strength should be largely free of interference such as the loss of fluorescence accompanied by sedimentation of Aβ(1−42) aggregates or light scattering by suspended Aβ(1−42) aggregates. Because of these advantages, competitive Cu(II) binding assays between this probe and Aβ(1−42) allowed us to observe a dramatic elevation of the apparent binding constant of Aβ(1−42) aggregates versus that of its monomeric counterpart. This finding is further supported by electron paramagnetic resonance (EPR) measurements of the sequestration of copper from HSA by Aβ(1−42) aggregates. The elevation in the copper binding strength could be rationalized by a structure in which three histidine residues from two different Aβ molecules and the C-terminal carboxylic group in the Aβ aggregates could also provide a substantially stronger copper coordination sphere that is otherwise unavailable in the Aβ monomers.

Table 1. Aβ Peptides Used in This Study and Their Sequences[a]

peptide	sequence
Aβ(1−16) (Y10W)	DAEFRHDSG**W**EVHHQK
Aβ(1−42)	DAEFRHDSGYEVHHQKLVFFAEDVGSNKGAI IGLMVGGVVIA

[a]The bold W indicates the mutation of Tyr-10 with Trp, and the hydrophobic segment of Aβ(1−42) is underlined.

METHODS

Chemicals and Reagents. Aβ(1−42) was obtained from American Peptide Co. Inc. (Sunnyvale, CA), and Aβ(1−16) and Aβ(1−16)(Y10W) were obtained from rPeptides Inc. (Bogart, GA). Aβ(1−16)(Y10W) synthesized in house with an automatic peptide synthesizer (Symphony Quartet, Tucson, AZ) was also used for some of the experiments. Acid- and globulin-free HSA (99% purity), sodium hydroxide, sulfuric acid, $CuCl_2$, copper acetate, 4-(2-hydroxyethyl)-1-piperazineethanesulfonic acid (HEPES), and other chemicals were acquired from Sigma-Aldrich (St. Louis, MO). All of the aqueous solutions were prepared using water purified by a Simplicity Water Purification System (Millipore, Bellerica, MA) to a resistivity of 18 MΩ cm.

Sample Preparation. Aβ(1−16) and Aβ(1−16)(Y10W) stock solutions (1−2 mM) were prepared by directly dissolving the lyophilized samples in 10 mM NaOH. They were then diluted with 10 mM HEPES buffer (pH 7.4) to desired concentrations. Prior to use, the Aβ(1−42) sample was treated with hexafluoro-2-propanol (HFIP) to dissolve any preexisting oligomers, and the solution was centrifuged for 30 min at 13000 rps to decant undissolved oligomers. The final solution was then lyophilized on a freeze-drier (VirTis Benchtop K, SP Scientific, Gardiner, NY). The Aβ(1−42) solutions were then prepared with our previously reported procedure.[8,9] Samples treated with the method by Teplow and co-workers[28] were also used and did not show obvious differences versus the HFIP-treated samples. The concentration of soluble peptides was determined with the UV−vis absorbance at 280 nm and the extinction coefficients of tryptophan [ε_{279} = 5400 cm M^{-1} for Aβ(1−16)(Y10W)] and tyrosine [ε_{276} = 1410 cm M^{-1} for Aβ(1−16) and Aβ(1−42)]. To avoid denaturation, a highly pure HSA sample (99%) was accurately weighed to prepare fresh and concentrated stock solutions, and mixtures of HSA, Cu(II), and various Aβ(1−42) peptides were used immediately for the competitive EPR assays. The Cu(II) stock solution was prepared by dissolving 1 mM $CuCl_2$ or copper acetate in a 1 mM H_2SO_4 solution.

Fluorescence Spectroscopy. Fluorescence measurements of Aβ(1−16) and Aβ(1−16)(Y10W) peptide solutions were taken at room temperature using a Cary Eclipse spectrofluorimeter (Agilent Technologies, Santa Clara, CA). An excitation wavelength (λ_{ex}) of 280 nm was used, and fluorescence intensities were recorded at 307 nm for Aβ and at 360 nm for Aβ(1−16)(Y10W). The entrance and exit slits were 10 and 5 nm, respectively. Fluorescence measurements were performed at least three times, and the standard deviations were plotted as the error bars. For determining apparent Cu(II) binding constants of aggregated Aβ(1−42), samples were prepared following two procedures. In the first procedure, 1.5 mL of 12.5 μM Aβ(1−42) was prepared and incubated in a 37 °C water bath. An aliquot was removed from the incubation solution and mixed with equimolar Aβ(1−16)(Y10W) and/or Cu(II) before the fluorescence intensities of Aβ(1−16)(Y10W) were measured. The final Aβ(1−16)(Y10W) and Cu(II) concentrations were both 12.5 μM, and the sampling times were 0 min, 20 min, 50 min, 3 h, 24 h, and 48 h. In the second procedure, 12.5 μM Cu(II) and 12.5 μM Aβ(1−42) in 1.2 mL of HEPES buffer were co-incubated. At different times of the incubation, aliquots of the mixture were withdrawn and mixed with 12.5 μM probe. The fluorescence intensity was monitored incrementally with a higher sampling frequency at the beginning of the aggregation. In both cases, to avoid light scattering by suspended aggregates during the fluorescence measurement, after the mixtures were allowed to stand for 10 min for equilibration, they were centrifuged and the supernatants were analyzed.

Atomic Force Microscopy. AFM images were obtained in air on an MFP-3D-SA microscope (Asylum Research, Santa Barbara, CA) equipped with the tapping mode. The AFM probes (MikroMasch, San Jose, CA) are single-beam cantilevers. Aliquots were taken out of an Aβ(1−42) solution or an Aβ(1−42)/Cu(II) mixture at predetermined incubation times, cast onto Ni(II)-treated mica sheets, and kept in contact with the mica sheets for 15 min. Afterward, the sheets were gently rinsed with water to remove salt and then dried with nitrogen.

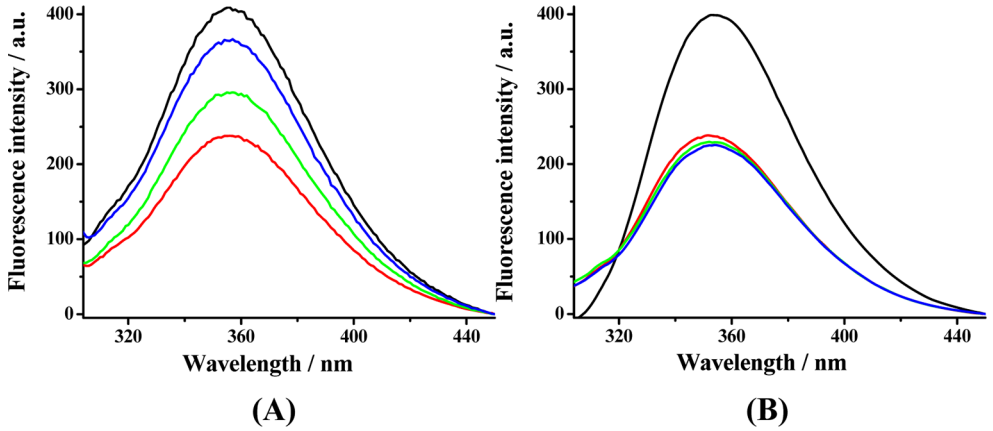

Figure 1. (A) Fluorescence spectra of the Aβ(1−16)(Y10W) probe without (black) and with additions of Cu(II) and aliquots of Aβ(1−42) taken from solutions incubated at 37 °C for 0 (red), 20 (green), and 1440 min (blue). (B) Control experiments using Aβ(1−16) instead of Aβ(1−42). The concentration of each species in the final solution was 12.5 μM.

Size Exclusion Chromatography. Size exclusion chromatography was performed with a Waters 600 HPLC system equipped with a photodiode array detector (model 2996). The mobile phase was 100 mM phosphate buffer (pH 7.4), and the flow rate was 0.2 mL/min. Two columns (GFC 2000 from Phenomenex Inc., Los Angeles, CA) were connected in series, and retention times were calibrated with the following five standards: blue dextran (2000 kDa), bovine serum albumin (66 kDa), chymotrypsinogen A (25 kDa), aprotinin (6.7 kDa), and vitamin B_{12} (1.35 kDa). From a 600 μL Aβ(1−42) solution incubated in a 37 °C water bath, a 20 μL aliquot was taken at each specific incubation time and then injected into the HPLC columns. Elution of Aβ species was monitored with the detector set at 220 nm.

Electron Paramagnetic Resonance Spectroscopy. EPR spectra were recorded using an X-band (~9.4 GHz) spectrometer (Elexsys E580) equipped with an HSQE resonator and a temperature controller (Oxford Instruments, Abingdon, England). EPR spectra were recorded at 123 K using N_2 gas flow with a microwave power of 1 mW and a modulation amplitude of 5 G. The concentration of Cu(II) bound by HSA at pH 7.4 is proportional to the integrated peak area in the continuous wave EPR absorption spectrum. A control experiment performed in a 60 μM HSA solution showed rather small Cu(II) EPR peaks [<5% of HSA fully loaded with Cu(II)], suggesting that the HSA samples we prepared were largely free of copper contamination. To ensure that free Cu(II) was absent in the mixture of HSA and Cu(II), the Cu(II)/HSA ratio was maintained at 0.8/1. The frozen sample proportionality constant for Cu^{2+} was determined via titrations of $CuCl_2$ with an excess of EDTA and 25% (v/v) glycerol. EPR spectra were baseline-corrected, and peaks were integrated with LabVIEW 7 Express (National Instruments, Austin, TX). A sample of 76 or 306 μM Aβ(1−42) was loaded in an EPR quartz tube (4 mm outside diameter and 3 mm inside diameter) and incubated for 6 and 24 h at 37 °C. The solution was then mixed with the Cu(II)−HSA complex. The Cu(II)−HSA complex was added to the preincubated Aβ(1−42) so that the final concentrations of HSA, Cu(II), and Aβ(1−42) were 61, 49, and 76 or 306 μM, respectively. All solutions were mixed thoroughly, sonicated for 2 min, and flash-frozen in liquid N_2.

RESULTS

Aβ(1−42) Aggregates Have a Substantially Elevated Copper Binding Strength in Comparison with That of the Monomer. The black curve in Figure 1A corresponds to the fluorescence spectrum of the Aβ(1−16)(Y10W) probe, which clearly exhibits an emission peak at 360 nm. With the addition of Cu(II), the Trp fluorescence of the probe is decreased (Figure S1A of the Supporting Information). This behavior is highly comparable to that of Aβ(1−16) and Aβ(1−42),[15,29] although the fluorescence signal is much stronger than the emissions of Aβ(1−16) and Aβ(1−42) at 307 nm. The Cu(II) binding constant of the probe can be measured by fitting the curve of fluorescence plotted versus Cu(II) concentration (cf. Figure S1B and details of the fitting procedure in the Supporting Information).[15,29] When an equimolar amount of a freshly prepared Aβ(1−42) sample was mixed with the probe and Cu(II), ~50% of the fluorescence was quenched (red curve in Figure 1A). This suggests that the Cu(II) ions are equally distributed between Aβ(1−42) and the probe. The equal distribution is understandable because the Cu(II) binding strength of the probe is similar to that of Aβ(1−42) (cf. Figure S1 of the Supporting Information and the description). Surprisingly, the fluorescence signal was partially recovered when Aβ(1−42) was preincubated for 20 min before being mixed with the probe (green curve in Figure 1A). More fluorescence recovery was observed after the Aβ(1−42) solution had been preincubated for a longer time [1440 min (blue curve in Figure 1A)]. In contrast, when the nonaggregating Aβ(1−16) sample was preincubated and then added to the solution, little recovery was observed (green and blue curves in Figure 1B). Because Aβ(1−42) is prone to rapid aggregation, the fluorescence recovery must have resulted from a stronger copper binding strength of Aβ(1−42) oligomers and other higher-order aggregates. To confirm the fidelity of using Aβ(1−16)(Y10W) to report on Cu(II) transfer, we added EDTA, a much stronger Cu(II) chelator, to a mixture of Aβ(1−16)(Y10W) and Cu(II) and observed a complete recovery of the probe fluorescence (Figure S2 of the Supporting Information). We therefore conclude from our experiments that, as the aggregation proceeds, Cu(II) initially bound by the probe is lost to the Aβ(1−42) aggregates.

dx.doi.org/10.1021/bi301053h | *Biochemistry* 2013, 52, 547−556

We can define the collective binding strength of all Aβ(1−42) species (monomers and aggregates) for Cu(II) with the apparent (overall) binding constant, K:

$$\text{A}\beta(1-42) + \text{Cu(II)} \overset{K}{\leftrightarrow} \text{A}\beta(1-42)-\text{Cu(II)} \quad (1)$$

$$\text{A}\beta(1-16)(\text{Y10W}) + \text{Cu(II)} \overset{K'}{\leftrightarrow} \text{A}\beta(1-16)(\text{Y10W})-\text{Cu(II)} \quad (2)$$

where K' is the Cu(II) binding constant of Aβ(1−16)(Y10W), which remains unchanged with time (cf. Figure S1 of the Supporting Information). Because the binding constant of HEPES with copper (pK = 3.22)[30] is 6 orders of magnitude smaller than that of the probe (pK = 9.49) and the Aβ peptides are in excess with respect to the Cu(II) concentration, the effect of HEPES buffer can be neglected.[31] Let θ_w be the percentage of Aβ(1−16)(Y10W) bound to Cu(II) and the initial (formal) concentrations of Aβ(1−42), Aβ(1−16)-(Y10W), and Cu(II) be A, L_0, and C, respectively. K is related to K' and θ_w as follows (cf. Supporting Information for the detailed derivation and the correction of the buffer effect in Figure S3):

$$K = \{[K'(1-\theta_w)(C-\theta_w L_0) - \theta_w)](1-\theta_w)K'\} / \{K'A\theta_w(1-\theta_w) - \theta_w[K'(1-\theta_w)(C-\theta_w L_0) - \theta_w]\} \quad (3)$$

At any given incubation time, θ_w can be readily obtained from the percentage of quenched fluorescence of the probe: $\theta_w = (F_0 - F_L)/F_0$, where F_0 is the fluorescence intensity of the probe-only solution and F_L the fluorescence intensity of the probe in a mixture. Although the apparent binding constant varies with the Aβ(1−42) aggregation or incubation time, the formal concentration of the Aβ(1−42) monomer at the inception of incubation is known. Hence, using eq 3, the apparent binding constant of a mixture of Aβ(1−42) aggregates and monomers can be accurately determined.

We took aliquots from an Aβ(1−42) solution incubated for different amounts of time and mixed them with the probe and Cu(II). Figure 2A reveals that the apparent binding constant of Aβ(1−42) aggregates has increased by ∼20 times over a 24 h incubation and more than 2 orders of magnitude (∼120) over a 48 h incubation.

Corresponding to the change in the apparent binding constant, atomic force microscopic (AFM) images (inset of Figure 2A) clearly display changes in the Aβ(1−42) aggregate morphology expected from the main Aβ(1−42) oligomerization−fibrillation pathway.[32−34] In this pathway, the aggregation process begins with the formation of globular oligomers (cf. AFM images for 20 and 50 min incubations), some of which subsequently transform into protofibrils (AFM image for a 180 min incubation) and fibrils (images for 1440 and 2880 min incubations). We also verified that the presence of Aβ(1−16)(Y10W) does not alter the Aβ(1−42) aggregation−fibrillation pathway (cf. Figure S4 of the Supporting Information). In addition, we followed the Aβ(1−42) aggregation−fibrillation process with the ThT assay (cf. Figure S5 of the Supporting Information). Notice that the plateau in Figure S5 of the Supporting Information (∼24 h) is consistent with the time when fibrils were observed by AFM (cf. the inset of Figure 2 at 1440 min). The trend depicted in Figure S5 of the Supporting Information is in contrast with that in Figure 2,

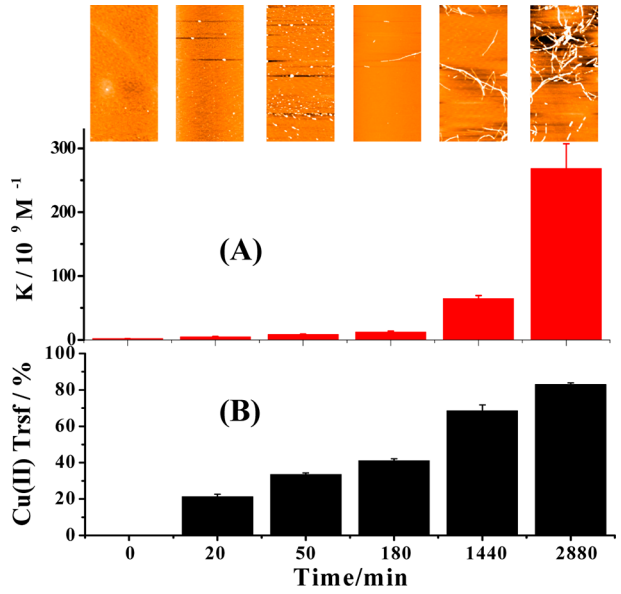

Figure 2. Changes in the apparent copper binding constant (A), morphology of Aβ(1−42) aggregates (inset), and distribution of copper (B) between the probe and Aβ(1−42) preincubated for different amounts of time. Cu(II) and the probe (12.5 μM each) were mixed with aliquots of Aβ(1−42) removed from a continuously incubated solution. The formal (initial) Aβ(1−42) concentration in the incubated solution was 12.5 μM. In panel B, the percentage of transfer is $(\theta_w^0 - \theta_w^t)/\theta_w^0$. The AFM images in the inset have areas of 5 μm × 2.5 μm.

which does not show a lag phase. Therefore, it is evident that oligomers formed soon after the incubation begin to bind Cu(II). Furthermore, oligomers, protofibrils, and fibrils of Aβ(1−42), with a conformation different from that of the natively unstructured Aβ(1−42) monomer, possess a substantially stronger Cu(II) binding strength. We also plotted the percentage of Cu(II) transferred from the probe to Aβ(1−42) over the entire incubation period (Figure 2B) to illustrate the extent of copper transfer resulting from the elevated copper binding strength.

While the AFM image (inset of Figure 2) of the sample incubated for 20 min shows only a few globular oligomers, Figure 2B indicates that a considerable amount of Cu(II) (∼20% of that originally bound by the probe) was lost. Thus, Cu(II) must be partially transferred to low-mass oligomers (i.e., dimers and pentamers), which are too small to be observed by AFM. The low-mass oligomers can be readily identified by size exclusion chromatography (Figure 3). Consistent with other reports,[32,35] the amount of soluble oligomers decreases with incubation time, while insoluble globular oligomers are formed as incubation prolongs (cf. the red and blue curves in Figure 3). Even after incubation for 1 day (yellow curve at 1440 min), a trace amount of monomers is still present in the solution, suggesting that Aβ fibrils remain in equilibrium with the monomeric Aβ. Overall, our results clearly indicate that the elevation of the Cu(II) binding strength in the incubated solution is proportional to the number of β-sheets inherent in all of the Aβ(1−42) oligomers (including the dimers) and aggregates.

Binding Constants of Aβ(1−42) at Different Incubation Times with Cu(II) Present Initially. We also co-incubated Cu(II) and Aβ(1−42) for different amounts of time. At predetermined incubation times, aliquots from this mixture

dx.doi.org/10.1021/bi301053h | *Biochemistry* 2013, 52, 547−556

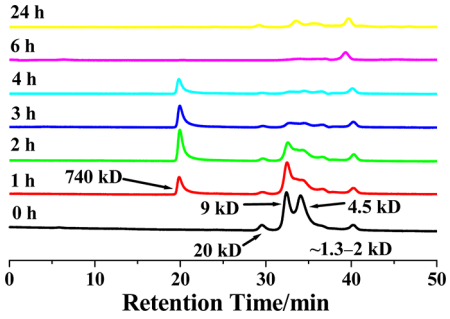

Figure 3. Size exclusion chromatograms of 80 μM Aβ(1−42) solutions incubated for different amounts of time, with the monomer (∼4.5 kDa), dimer (∼9 kDa), pentamer (∼20 kDa), and a soluble oligomer (740 kDa) identified. The small peak corresponding to 1.3−2 kDa was verified by mass spectrometry as a cluster of minor impurities in the synthetic Aβ(1−42) sample. Notice that during the ∼40 min separation of a fresh Aβ(1−42) solution (i.e., no incubation), a noticeable amount of dimers and pentamers had already formed.

were withdrawn and mixed with the probe for fluorescence measurements. Figure 4 shows the changes in the copper

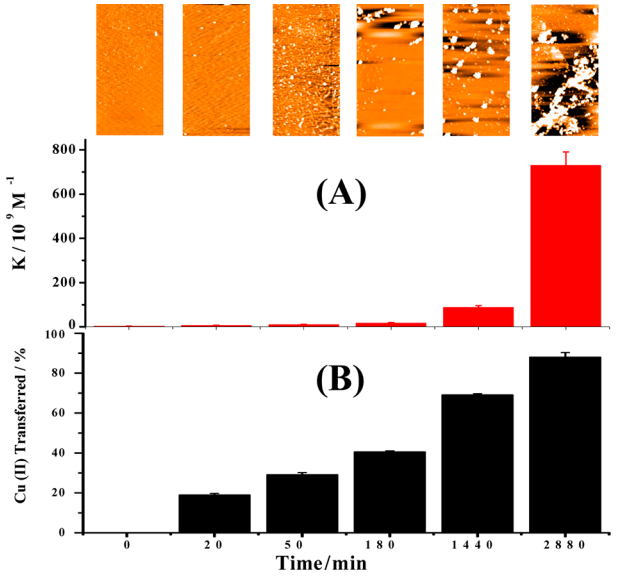

Figure 4. Changes in the copper binding strength, morphology of the aggregates, and distribution of copper between the probe and Aβ(1−42) incubated for different amounts of time. (A) K values of Aβ(1−42) at various incubation times when Cu(II) was present from the beginning. Equimolar amounts (12.5 μM) of Aβ(1−42) and Cu(II) were first mixed and incubated at 37 °C for different amounts of time. At different times aliquots of the mixture were withdrawn and mixed with 12.5 μM Aβ(1−16)(Y10W) for measurement. (B) Percentages of Cu(II) transferred from the probe to Aβ(1−42) at different incubation times. The inset shows aggregates imaged by AFM at the corresponding incubation times (image area of 5 μm × 2.5 μm).

binding strength obtained by processing the fluorescence recovery data, together with the AFM images of the aggregates and distribution of copper between the probe and Aβ(1−42). Remarkably, both the trend and extent of changes in the K values (Figure 4A) are analogous to those in Figure 2A, even though amorphous aggregates are the predominate species at and beyond incubation for 3 h (inset of Figure 4A). Our observation is consistent with the previous finding that binding of copper to Aβ(1−42) alters the main aggregation pathway of Aβ(1−42) from fibrillation to the formation of amorphous aggregates.[36] Nevertheless, the comparability of the K values deduced at intermediate and extended incubation times between Figures 2A and 4A suggests that the amorphous aggregates bind to Cu(II) almost as strongly as protofibrils and fibrils. Despite the current debate regarding whether fibrils evolve out of amorphous intermediates[37] or are produced as a result of stacking of oligomers,[37] it is believed that amorphous aggregates contain misfolded and β-sheet-rich Aβ(1−42) molecules.[38] Again, the results in Figure 4 support our earlier contention that formation of β-sheets during Aβ(1−42) aggregation is crucial to the elevation of the copper binding strength. We also conducted an experiment by continuously monitoring the fluorescence signals in a single solution of Cu(II), Aβ(1−16)(Y10W), and Aβ(1−42). The fluorescence recovery monitored as a function of incubation time is shown in Figure S6 of the Supporting Information. The good comparability between Figure 4A and Figure S6 of the Supporting Information suggests that Aβ(1−16)(Y10W) does not alter the interaction of Cu(II) with the Aβ(1−42) monomer and aggregates. In a separate experiment, we found that co-incubating Aβ(1−16)(Y10W) with Aβ(1−42) and Cu(II) does not alter the Aβ(1−42) aggregation pathway [i.e., amorphous aggregate formation caused by Cu(II) (cf. Figure S7 of the Supporting Information)]. However, monitoring the fluorescence recovery in a single solution prevents us from centrifuging the solution to remove large aggregates that can scatter light. As a consequence, light scattering (much like in the fluorescence scattering measurement of aggregation of amyloidogenic molecules[34]) is more serious in the solution beyond 24 h. Thus, we believe that the apparent binding constants deduced from Figure 4A are more reliable. Finally, we should add that, if all of the monomers in the incubated solution had been converted into fibrils or amorphous aggregates, the K values would be even greater than those shown in Figure 2 or 4. Because in the yellow curve of Figure 3 monomers were still observed after incubation for 24 h, it is clear that the incubated solutions used to obtain Figures 2 and 4 were mixtures of Aβ(1−42) monomers, oligomers, and large aggregates.

Table 2. EPR Parameters Extracted from Figure 5

sample	description	$A_\parallel$ (G)[a]	$g_\parallel$[a]	$g_\perp$
A	Cu(II)−HSA	182 (1)	2.160 (1)	2.052
B	freshly prepared Aβ(1−42) and Cu(II)−HSA	182 (1)	2.160 (1)	2.052
C	Aβ(1−16) and Cu(II)−HSA	182 (1)	2.159 (1)	2.052
D	Cu(II)−HSA and aggregated Aβ(1−42) (incubation for 6 h)	182 (1) 168 (2)	2.161 (1) 2.275 (2)	2.055
E	Cu(II) and aggregated Aβ(1−42) (incubated for 6 h)	168 (2)	2.278 (2)	2.059

[a]The numbers in parentheses denote components 1 and 2.

Aβ(1−42) Aggregates Are Capable of Sequestering Cu(II) from HSA. With electron paramagnetic resonance (EPR), we investigated whether any transfer of Cu(II) from HSA to Aβ aggregates is possible. Shown on the left of Figure 5 are EPR spectra of the Cu(II)−HSA complex (curve A), a freshly prepared Aβ(1−42) solution mixed with the Cu(II)−HSA complex (curve B), and the Cu(II)−HSA complex mixed with Aβ(1−16) (curve C). We have also obtained an EPR spectrum from a solution comprising the Cu(II)−HSA

dx.doi.org/10.1021/bi301053h | *Biochemistry* 2013, 52, 547−556

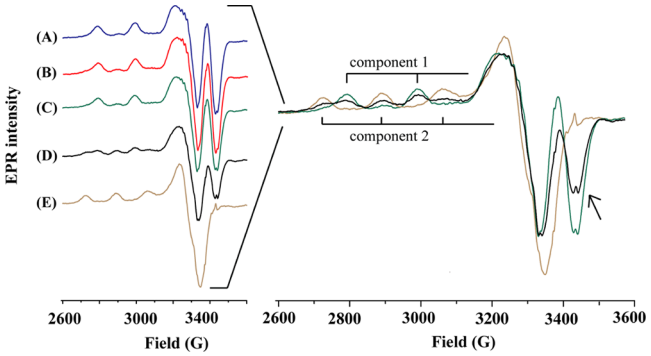

Figure 5. EPR spectra (left) of (A) the Cu(II)−HSA complex, (B) a mixture of the Cu(II)−HSA complex and freshly prepared Aβ(1−42), (C) a mixture of the Cu(II)−HSA complex and Aβ(1−16), (D) a mixture of the Cu(II)−HSA complex and Aβ(1−42) aggregates (incubation for 6 h), and (E) the complex formed between Cu(II) and aggregated Aβ(1−42) (incubation for 6 h). Overlay of spectra A, D, and E (right) with the hyperfine peaks of the Cu(II)−Aβ(1−42) complex denoted as component 2 and those of the Cu(II)−HSA complex as component 1. The arrow indicates the decrease in the magnitude of the negative peak at 3423 G. The concentrations of Cu(II), HSA, and Aβ were 49, 61, and 306 μM, respectively. Aggregation of Aβ(1−42) was performed by placing the sample inside the EPR tube and incubating it at 37 °C for 6 h.

complex and preformed Aβ(1−42) oligomers and protofibrils (curve D) as well as a spectrum of Cu(II) complexed with Aβ(1−42) oligomers and protofibrils (curve E). The right panel of Figure 5 is an overlay of EPR spectra A, D, and E, which clearly exhibits the differences in $g_\perp$ and $g_\parallel$ peaks among the three solutions. The line shape of and parameters calculated from curve A ($g_\parallel$ = 2.160 and $A_\parallel$ = 182 G for component 1) are consistent with those previously reported for the Cu(II)−HSA complex,[24,39,40] with two negative peaks at 3329 and 3423 G and two distinctive hyperfine peaks. Notice that curves B and C are highly comparable to curve A, suggesting that neither Aβ(1−16) nor the Aβ(1−42) monomer can remove Cu(II) from HSA, a result expected from the aforementioned large difference in the binding strengths between monomeric Aβ and HSA. These data are also in line with the report by Faller's group that showed that both monomeric Aβ(1−40) and Aβ(1−16) cannot seize Cu(II) from HSA.[24] However, with the addition of a preincubated Aβ(1−42) solution to a solution of the Cu(II)−HSA complex, the magnitude of the negative peak at 3329 G increases at the expense of the magnitude of the negative peak at 3423 G (cf. right panel of Figure 5), concurrent with the appearance of three new hyperfine peaks ($g_\parallel$ = 2.275 and $A_\parallel$ = 168 G; cf. curve D for component 2 in the right panel of Figure 5). The parameters of these new peaks are consistent with those of the copper complex of aggregated Aβ(1−42) shown in curve E.[41,42] Therefore, our data clearly demonstrate that a preincubated Aβ(1−42) sample can sequester copper from the Cu(II)−HSA complex.

We also estimated the copper binding constant (K) of aggregated Aβ(1−42) by deconvoluting the two components in curve D to yield a ratio of Cu(II) bound to HSA over that complexed by the Aβ(1−42) aggregates. An increase in the copper binding strength of ∼1 order of magnitude was observed for Aβ(1−42) aggregates after a 6 h incubation (Table S2 of the Supporting Information), consistent with the results obtained by our fluorescence measurement. Both the EPR spectra shown in Figure 5 and the binding constants estimated from the competitive EPR assay (Table S2) have unequivocally validated the significantly elevated copper binding strength of aggregated Aβ(1−42).

Finally, the affinity constants we measured reflect only average affinity of all Aβ(1−42) species in the incubated sample. The true Cu(II) sequestration power of the Aβ(1−42) fibrils should be even stronger than the affinity measured for Aβ(1−42) after 48 h of incubation. Notice that in Figure 2A, the dissociation constant converted from the K value at 2880 min is ∼3 pM, which is close to the K_d value of the Cu(II)−HSA complex.[21] In Figure 5, the changes in the EPR spectra and parameters are likely to be caused solely by the Aβ(1−42) fibrils whose actual K_d value should be less than 3 pM.

DISCUSSION

Employing two independent methods (fluorescence and EPR competitive binding assays), we demonstrate that Aβ(1−42) oligomers and aggregates bind copper more strongly than their monomeric counterpart. Our finding contradicts the recent study by Sarell et al., who reported a dissociation constant (K_d) of ∼60 pM for both monomeric and aggregated Aβ(1−42).[18] Such a K_d value is at least more than 1 order of magnitude lower than values reported by many other studies for Aβ monomers even after buffer correction (see Table S1 of the Supporting Information). As shown by our comparative studies detailed in the Supporting Information (cf. Figures S8−S10), the discrepancy stems from the uncertainties inherent in the Tyr-10 fluorescence measurement as well as in the sample preparative method. Specifically, changes in the Tyr-10 fluorescence of Aβ(1−42) at 307 nm can be caused by both Cu(II) binding and the precipitation and suspension of the Cu(II)-containing Aβ(1−42) aggregates in solution. The effects of the aggregate precipitation and suspension are particularly acute when large and insoluble aggregates are formed. The former process decreases the fluorescence intensity, while the latter process scatters light to cause signal fluctuation. When the relatively weak Tyr fluorescence is quenched to a low level, the interference of the adjacent Raman peak of water (313 nm) becomes more pronounced (cf. Figure S10A of the Supporting Information) and can also affect the accurate measurement of the fluorescence intensity. Our method allows the removal of the Cu(II)-containing Aβ(1−42) aggregates prior to the fluorescence measurements. Moreover, the fluorescence quantum yield of Trp is much higher than that of Tyr, and Trp fluoresces at a longer wavelength. Consequently, the water Raman peak does not interfere (cf. Figure S10B of the Supporting Information) with the fluorescence of the Aβ(1−16)(Y10W) probe. We should also caution that sample pretreatment is crucial to the accurate measurement of the Cu(II) binding affinity values of Aβ(1−42). We noticed that the pretreatment procedure employed in the work of Viles and co-workers is different from procedures used by other studies.[18] We found that after such a pretreatment Aβ(1−42) samples generally contain a large number of oligomers (cf. Figure S8 of the Supporting Information). These samples exhibit behavior different from the behavior of those treated with the HFIP method.[28,43] As shown in Figure S9 of the Supporting Information, the presence of oligomers at the beginning of Cu(II) addition results in the appearance of a higher Cu(II) binding strength. In other words, if in the initial solution oligomers are present at a high concentration, there will be little difference in the binding affinity values between the presumed "Aβ(1−42) monomers" and the actual oligomers. This factor,

dx.doi.org/10.1021/bi301053h | *Biochemistry* 2013, 52, 547−556

together with effects from other experimental conditions (buffer, pH, concentrations of competitive ligands, etc.; cf. the comprehensive review by Faller and co-workers[31]), must be taken into account in deducing the final affinity constants.

The metal binding strength increase in oligomers (including dimer), and other higher-order aggregates of Aβ(1−42) most likely originate from a tighter coordination structure that cannot be rendered by the monomer. His-6, His-13, and His-14 and the N-terminus are the four N-containing moieties that account for the 3N1O coordination sphere identified by EPR in the Cu(II) complex of the Aβ monomer.[44,45] Because His-13 and His-14 are adjacent to each other, they are on the opposite sides of the peptide backbone. Such an orientation prevents them from simultaneously participating in a tight Cu(II) binding when only one Aβ(1−42) monomer is involved.[44,46] Aβ(1−42) dimers are formed with a β-sheet comprising two pairs of β-strands withheld by hydrogen bonding.[47,48] Consequently, all of the metal binding sites are located in the N-termini that extend out of the β-sheet. Larger oligomers, protofibrils, and fibrils are produced from stacking of the β-sheet-containing oligomers (or "aggregation units"),[49,50] again positioning all of the hydrophilic N-termini on the same side of the stacked β-sheets.[49] Although amorphous aggregates lack higher regularity for ordered β-sheet stacking, they have been shown to contain many β-sheets.[38] Therefore, a plausible cause for the enhanced Cu(II) binding strength in both ordered and amorphous Aβ aggregates is that more histidine residues (one of the strongest metal-binding ligands among amino acid residues[51]) have become available for Cu(II) binding and are favorably spaced out to coordinate Cu(II). Binding by three histidine residues is a more stable configuration than those in other modes.[52] As shown in our proposed model (Figure 6), upon aggregation His-13 in one Aβ molecule and His-14 from another can concurrently coordinate Cu(II), tightly locking the Cu(II) ion in position. In addition, the C-terminal carboxylic group is folded back and has been shown to provide additional ligation.[52] Such a Cu(II) coordination sphere is also unlikely to exist in the monomeric form. Other possibilities can also contribute to the enhanced Cu(II) binding. For example, the ligand crowding caused by β-sheet formation could allow some amide groups or other dangling carboxylic groups to participate in additional binding. We also cannot rule out the possibility that the increase in binding strength is caused by the change near the copper center from a more hydrophilic environment in the Aβ monomers to the more hydrophobic setting in the Aβ aggregates. The rather small increase (almost within experimental error) in the Zn(II) binding strength from Aβ monomers to aggregates[26,27] might also result from one or more of the factors mentioned above.

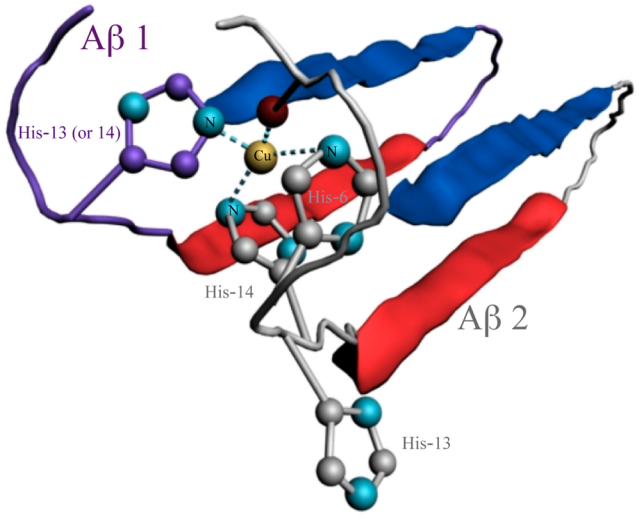

Figure 6. Model proposed for the Cu(II) coordination sphere in Aβ(1−42) oligomers and higher-order aggregates. Histidine residues from two different Aβ(1−42) molecules (denoted Aβ1 and Aβ2) provide three of the four Cu(II)-binding ligands. One histidine is colored purple, while the other two in an adjacent Aβ(1−42) molecule in the same aggregate are colored gray.

The intermolecular coordination model posited above is supported by a growing body of evidence. For example, Pedersen et al. suggested that, unlike soluble Aβ(1−16), Aβ(1−40), which is also prone to β-sheet formation and aggregation, could rapidly form the Aβ−Cu(II)−Aβ linkage prior to oligomerization.[53] We hypothesize that such a linkage might be preserved in the copper-complexing Aβ(1−42) oligomers and aggregates. Szalai and co-workers, using X-ray absorption spectroscopy, demonstrated that the Cu(II) coordination sphere in oligomers is different from that in monomers. Specifically, only two histidines participate in Cu(II) binding, whereas three histidines are involved in the coordination of copper by Aβ oligomers[54] (even though it is not clear whether the three histidines are from the same or different Aβ molecules). From the study presented here, it is evident that the rapid formation of small, soluble oligomers (cf. chromatograms in Figure 3) synchronizes with the transfer of copper from the probe to Aβ(1−42) aggregates.

The significantly elevated Cu(II) binding strength of Aβ aggregates has two major biological implications. First, it has long been proposed that overproduction of Aβ peptides (e.g., in the case of early onset AD[55]) and inefficient clearance are at least partially responsible for the accumulation and deposition of Aβ and aggregation of Aβ in vivo. Even when the regulation of cellular Cu(II) is normal, the higher Cu(II) binding strength inherent in Aβ oligomers and fibrils due to Aβ overproduction and/or inefficient clearance would facilitate and aggravate sequestration of Cu(II) from copper-transporting proteins such as HSA, which may explain why a high level of copper exists in senile plaques.

The second implication is related to the high toxicity of diffusible oligomers of Aβ[56,57] and their enhanced copper binding strength. In normal brain, the Aβ monomer and its oligomeric forms are in an equilibrium and their relative abundance is dependent on how each species is metabolized (cleared). When copper homeostasis is disrupted in AD,[58] excess copper[59] in the cellular milieu is capable of binding Aβ oligomers and stabilizing the Aβ aggregates. Consequently, the equilibrium between the Aβ monomer and its aggregates is shifted to the direction of Aβ oligomerization and aggregation. Because the Aβ−Cu(II) complex catalyzes the generation of ROS,[5,9,10] the copper-containing oligomers could potentially behave as a mobile ROS generator, leading to an extensive oxidative stress that is commonly found in AD brain.[14,60] Given the significant role of albumin in regulating copper in normal brain and the possible link between albumin deficiency and AD development,[40,61,62] in vivo Aβ aggregation may be triggered by albumin deficiency and/or its weaker copper chelating capacity.[59,63] This is supported by an interesting fact that 60−90% of AD cases are associated with cerebral ischemia,[64,65] which has been shown to decrease the metal binding capacity of

dx.doi.org/10.1021/bi301053h | *Biochemistry* 2013, 52, 547−556

albumin.[66] As a consequence, transfer of copper from albumin to Aβ aggregates is likely to be favored. Indeed, treatment of AD patients with plasma exchange, in which their albumin is replaced with that in donors' plasma, is undergoing clinical trials and has shown promising results.[67]

CONCLUSION

In summary, our fluorescence and EPR measurements both clearly demonstrate that Aβ(1−42) oligomers and aggregates bind copper much more strongly than their monomeric counterpart. The novel application of a highly fluorescent, Aβ-derived probe allowed us to interrogate the increasing extent of copper sequestration by aggregating Aβ(1−42) species. The Aβ(1−16)(Y10W) probe also mitigates uncertainties inherent in the use of the intrinsic Tyr-10 fluorescence of Aβ peptides for Cu(II) binding studies. The discovery of the aggregation-dependent copper binding of Aβ(1−42) suggests that Aβ(1−42) aggregates could be the species that lead to accumulation of copper and possibly other metals in senile plaques. The elevated Cu(II) binding strength of Aβ(1−42) aggregates strengthens the hypothesis of copper-induced oxidative stress in AD. Results from this study also manifest the importance of intact albumin and a possible linkage between disruption of copper homeostasis and AD pathology.

ASSOCIATED CONTENT

Supporting Information

Detailed derivation of eq 3, measurement of the K_a of Aβ(1−16)(Y10W), effects of Aβ(1−42) sample treatments and the fluorescence measurement of Tyr-10 on the accuracy of the K_a values, and a table listing K_a values of representative Aβ peptides. This material is available free of charge via the Internet at http://pubs.acs.org.

AUTHOR INFORMATION

Corresponding Author

*Phone: (323) 343-2390. Fax: (323) 343-6490. E-mail: fzhou@calstatela.edu.

Author Contributions

D.J. and L.Z. contributed equally to this work.

Funding

The work is partially supported by the National Institutes of Health (SC1NS070155-01 to F.Z. and GM065790 to G.L.M.) and a National Science Foundation Research in Undergraduate Institutions grant (1112105 to F.Z.).

Notes

The authors declare no competing financial interest.

ACKNOWLEDGMENTS

A portion of this research was performed with help from Dr. Eric Walter using EMSL, a national scientific user facility sponsored by the Department of Energy's Office of Biological and Environmental Research and located in the Pacific Northwest National Laboratory. We gratefully acknowledge Dr. Peter Z. Qin for the access to the EPR instrument at the University of Southern California (Los Angeles, CA). We also thank Mr. Ding Li for drawing the model shown in Figure 6.

ABBREVIATIONS

Aβ, amyloid-β; AD, Alzheimer's disease; ROS, reactive oxygen species; CSF, cerebrospinal fluid; HSA, human serum albumin; EPR, electron paramagnetic resonance; HEPES, 4-(2-hydroxyethyl)-1-piperazineethanesulfonic acid; AFM, atomic force microscopy.

REFERENCES

(1) Selkoe, D. J. (2002) Alzheimer's disease is a synaptic failure. *Science 298* (5594), 789−791.

(2) Hardy, J. A., and Higgins, G. A. (1992) Alzheimer's disease: The amyloid cascade hypothesis. *Science 256*, 184−185.

(3) Lovell, M. A., Robertson, J. D., Teesdale, W. J., Campbell, J. L., and Markesbery, W. R. (1998) Copper, iron and zinc in Alzheimer's disease senile plaques. *J. Neurol. Sci. 158*, 47−52.

(4) Smith, D. P., Smith, D. G., Curtain, C. C., Boas, J. F., Pilbrow, J. R., Ciccotosto, G. D., Lau, T.-L., Tew, D. J., Perez, K., Wade, J. D., Bush, A. I., Drew, S. C., Separovic, F., Masters, C. L., Cappai, R., and Barnham, K. J. (2006) Copper-mediated amyloid-β toxicity is associated with an intermolecular histidine bridge. *J. Biol. Chem. 281*, 15145−15154.

(5) Huang, X. D., Cuajungco, M. P., Atwood, C. S., Hartshorn, M. A., Tyndall, J. D. A., Hanson, G. R., Stokes, K. C., Leopold, M., Multhaup, G., Goldstein, L. E., Scarpa, R. C., Saunders, A. J., Lim, J., Moir, R. D., Glabe, C., Bowden, E. F., Masters, C. L., Fairlie, D. P., Tanzi, R. E., and Bush, A. I. (1999) Cu(II) potentiation of Alzheimer Aβ neurotoxicity: Correlation with cell-free hydrogen peroxide production and metal reduction. *J. Biol. Chem. 274*, 37111−37116.

(6) Cherny, R. A., Atwood, C. S., Xilinas, M. E., Gray, D. N., Jones, W. D., McLean, C. A., Barnham, K. J., Volitakis, I., Fraser, F. W., Kim, Y.-S., Huang, X., Goldstein, L. E., Moir, R. D., Lim, J. T., Beyreuther, K., Zheng, H., Tanzi, R. E., Masters, C. L., and Bush, A. I. (2001) Treatment with a copper-zinc chelator markedly and rapidly inhibits β-amyloid accumulation in Alzheimer's disease transgenic mice. *Neuron 30*, 665−676.

(7) Sparks, D. L., and Schreurs, B. G. (2003) Trace amounts of copper in water induce β-amyloid plaques and learning deficits in a rabbit model of Alzheimer's disease. *Proc. Natl. Acad. Sci. U.S.A. 100*, 11065−11069.

(8) Jiang, D., Li, X., Liu, L., Yagnik, G. B., and Zhou, F. (2010) Reaction rates and mechanism of the ascorbic acid oxidation by molecular oxygen facilitated by Cu(II)-containing amyloid-β complexes and aggregates. *J. Phys. Chem. B 114*, 4896−4903.

(9) Jiang, D., Men, L., Wang, J., Zhang, Y., Chickenyen, S., Wang, Y., and Zhou, F. (2007) Redox reactions of copper complexes formed with different β-amyloid peptides and their neuropathalogical relevance. *Biochemistry 46*, 9270−9282.

(10) Guilloreau, L., Combalbert, S., Sournia-saquet, A., Mazarguil, H., and Faller, P. (2007) Redox chemistry of copper-amyloid-β: The generation of hydroxyl radical in the presence of ascorbate is linked to redox-potentials and aggregation state. *ChemBioChem 8*, 1317−1325.

(11) Hewitt, N., and Rauk, A. (2009) Mechanism of hydrogen peroxide production by copper-bound amyloid β peptide: A theoretical study. *J. Phys. Chem. B 113*, 1202−1209.

(12) Hureau, C., Coppel, Y., Dorlet, P., Solari, P. L., Sayen, S., Guillon, E., Sabater, L., and Faller, P. (2009) Deprotonation of the Asp1-Ala2 peptide bond induces modification of the dynamic copper(II) environment in the amyloid-β peptide near physiological pH. *Angew. Chem., Int. Ed. 48*, 9522−9525.

(13) Drew, S. C., Noble, C. J., Masters, C. L., Hanson, G. R., and Barnham, K. J. (2009) Pleomorphic Copper Coordination by Alzheimer's Disease Amyloid-β Peptide. *J. Am. Chem. Soc. 131*, 1195−1207.

(14) Dong, J., Atwood, C. S., Anderson, V. E., Siedlak, S. L., Smith, M. A., Perry, G., and Carey, P. R. (2003) Metal binding and oxidation of amyloid-β within isolated senile plaque cores: Raman microscopic evidence. *Biochemistry 42*, 2768−2773.

(15) Maiti, N., Jiang, D., Wain, A. J., Patel, S., Dinh, K. L., and Zhou, F. (2008) Mechanistic studies of Cu(II) binding to amyloid-β peptides and the fluorescence and redox behaviors of the resulting complexes. *J. Phys. Chem. B 112*, 8406−8411.

(16) Guilloreau, L., Damian, L., Coppel, Y., Mazarguil, H., Winterhalter, M., and Faller, P. (2006) Structural and thermodynamical properties of Cu-II amyloid-β 16/28 complexes associated with Alzheimer's disease. *J. Biol. Inorg. Chem. 11*, 1024−1038.
(17) Hong, L., Bush, W. D., Hatcher, L. Q., and Simon, J. (2008) Determining thermodynamic parameters from isothermal calorimetric isotherms of the binding of macromolecules to metal cations originally chelated by a weak ligand. *J. Phys. Chem. B 112*, 604−611.
(18) Sarell, C. J., Syme, C. D., Rigby, S. E. J., and Viles, J. H. (2009) Copper(II) binding to amyloid-β fibrils of Alzheimer's disease reveals a picomolar affinity: Stoichiometry and coordination geometry are independent of Aβ oligomeric form. *Biochemistry 48*, 4388−4402.
(19) Linder, M. C. (1991) *Biochemistry of copper*, Plenum Press, New York.
(20) Laussac, J. P., and Sarkar, B. (1984) Characterization of the copper(II) and nickel(II) transport site of human serum albumin. Studies of copper(II) and nickel(II) binding to peptide 1−24 of human serum albumin by carbon-13 and proton NMR spectroscopy. *Biochemistry 23*, 2832−2838.
(21) Rózga, M., Sokołowska, M., Protas, A. M., and Bal, W. (2007) Human serum albumin coordinates Cu(II) at its N-terminal binding site with 1 pM affinity. *J. Biol. Inorg. Chem. 12*, 913−918.
(22) Masuoka, J., and Saltman, P. (1994) Zinc(II) and copper(II) binding to serum albumin. A comparative study of dog, bovine, and human albumin. *J. Biol. Chem. 269*, 25557−25561.
(23) Ida, N., Hartmann, T., Pantel, J., Schröder, J., Zerfass, R., Förstl, H., Sandbrink, R., Masters, C. L., and Beyreuther, K. (1996) Analysis of heterogeneous βA4 peptides in human cerebrospinal fluid and blood by a newly developed sensitive Western blot assay. *J. Biol. Chem. 271*, 22908−22914.
(24) Perrone, L., Mothes, E., Vignes, M., Mockel, A., Figueroa, C., Miquel, M.-C., Maddelein, M.-L., and Faller, P. (2010) Copper transfer from Cu-Aβ to human serum albumin inhibits aggregation, radical production and reduces Aβ toxicity. *ChemBioChem 11*, 110−118.
(25) Cherny, R. A., Legg, J. T., McLean, C. A., Fairlie, D. P., Huang, X., Atwood, C. S., Beyreuther, K., Tanzi, R. E., Masters, C. L., and Bush, A. I. (1999) Aqueous dissolution of Alzheimer's disease Aβ amyloid deposits by biometal depletion. *J. Biol. Chem. 274*, 23223−23228.
(26) Talmard, C., Bouzan, A., and Faller, P. (2007) Zinc binding to amyloid-β: Isothermal titration calorimetry and Zn competition experiments with Zn sensors. *Biochemistry 46*, 13658−13666.
(27) Tõugu, V., Karafin, A., and Palumaa, P. (2008) Binding of zinc(II) and copper(II) to the full-length Alzheimer's amyloid-β peptide. *J. Neurochem. 104*, 1249−1259.
(28) Fezoui, Y., Hartley, D. M., Harper, J. D., Khurana, R., Walsh, D. M., Condron, M. M., Selkoe, D. J., Lansbury, P. T., Jr., Fink, A. L., and Teplow, D. B. (2000) An improved method of preparing the amyloid β-protein for fibrillogenesis and neurotoxicity experiments. *Amyloid 7*, 166−178.
(29) Syme, C. D., Nadal, R. C., Rigby, S. E. J., and Viles, J. H. (2004) Copper binding to the amyloid-β (Aβ) peptide associated with Alzheimer's disease. *J. Biol. Chem. 279*, 18169−18177.
(30) Sokołowska, M., and Bal, W. (2005) Cu(II) complexation by "non-coordinating" N-2-hydroxyethylpiperazine-N′-2-ethanesulfonic acid (HEPES buffer). *J. Inorg. Biochem. 99*, 1653−1660.
(31) Faller, P., and Hureau, C. (2009) Bioinorganic chemistry of copper and zinc ions coordinated to amyloid-β peptide. *Dalton Trans.*, 1080−1094.
(32) Lee, J., Culyba, E. K., Powers, E. T., and Kelly, J. W. (2011) Amyloid-β forms fibrils by nucleated conformational conversion of oligomers. *Nat. Chem. Biol. 7* (9), 602−609.
(33) Jarrett, J. T., and Lansbury, P. T., Jr. (1993) Seeding "one-dimensional crystallization" of amyloid: A pathogenic mechanism in Alzheimer's disease and scrapie. *Cell 73*, 1055−1058.
(34) Bitan, G., Kirkitadze, M. D., Lomakin, A., Vollers, S. S., Benedek, G. B., and Teplow, D. B. (2003) Amyloid β-protein (Aβ) assembly: Aβ40 and Aβ42 oligomerize through distinct pathways. *Proc. Natl. Acad. Sci. U.S.A. 100*, 330−335.
(35) Bush, A. I., Pettingell, W. H., Jr., Paradis, M. D., and Tanzi, R. E. (1994) Modulation of Aβ adhesiveness and secretase site cleavage by zinc. *J. Biol. Chem. 269*, 12152−12158.
(36) Ryu, J., Girigoswami, K., Ha, C., Ku, S. H., and Park, C. B. (2008) Influence of multiple metal ions on β-amyloid aggregation and dissociation on a solid surface. *Biochemistry 47* (19), 5328−5335.
(37) Liang, Y., Lynn, D. G., and Berland, K. M. (2010) Direct observation of nucleation and growth in amyloid self-assembly. *J. Am. Chem. Soc. 132*, 6306−6308.
(38) Maurer-Stroh, S., Debulpaep, M., Kuemmerer, N., Lopez de la Paz, M., Martins, I. C., Reumers, J., Morris, K. L., Copland, A., Serpell, L., Serrano, L., Schymkowitz, J. W., and Rousseau, F. (2010) Exploring the sequence determinants of amyloid structure using position-specific scoring matrices. *Nat. Methods 7*, 237−242.
(39) Valko, M., Morris, H., Mazúr, M., Telser, J., McInnes, E. J. L., and Mabbs, F. E. (1999) High-affinity binding site for copper(II) in human and dog serum albumins (an EPR study). *J. Phys. Chem. B 103*, 5591−5597.
(40) Bal, W., Christodoulou, J., Sadler, P. J., and Tucker, A. (1998) Multi-metal binding site of serum albumin. *J. Inorg. Biochem. 70*, 33−39.
(41) Karr, J. W., Kaupp, L. J., and Szalai, V. A. (2004) Amyloid-β binds Cu^{2+} in a mononuclear metal ion binding site. *J. Am. Chem. Soc. 126*, 13534−13538.
(42) Karr, J. W., and Szalai, V. A. (2008) Cu(II) binding to monomeric, oligomeric, and fibrillar forms of the Alzheimer's disease amyloid-β peptide. *Biochemistry 47* (17), 5006−5016.
(43) Karr, J. W., Akintoye, H., Kaupp, L. J., and Szalai, V. A. (2005) N-terminal deletions modify the Cu^{2+} binding site in amyloid-β. *Biochemistry 44*, 5478−5487.
(44) El Khoury, Y., Dorlet, P., Faller, P., and Hellwig, P. (2011) New insights into the coordination of Cu(II) by the amyloid-β 16 peptide from Fourier transform IR spectroscopy and isotopic labeling. *J. Phys. Chem. B 115*, 14812−14821.
(45) Karr, J. W., and Szalai, V. A. (2007) Roles of aspartate-1 in Cu(II) binding to the amyloid-β peptide of Alzheimer's disease. *J. Am. Chem. Soc. 129*, 3796−3797.
(46) Shin, B.-K., and Saxena, S. (2011) Substantial contribution of the two imidazole rings of the His13-His14 dyad to Cu(II) binding in amyloid-β(1−16) at physiological pH and its significance. *J. Phys. Chem. A 115*, 9590−9602.
(47) Yamaguchi, T., Yagi, H., Goto, Y., Matsuzaki, K., and Hoshino, M. (2010) A disulfide-linked amyloid-β peptide dimer forms a protofibril-like oligomer through a distinct pathway from amyloid fibril formation. *Biochemistry 49*, 7100−7107.
(48) Hwang, W., Zhang, S., Kamm, R. D., and Karplus, M. (2004) Kinetic control of dimer structure formation in amyloid fibrillogenesis. *Proc. Natl. Acad. Sci. U.S.A. 101*, 12916−12921.
(49) Lührs, T., Ritter, C., Adrian, M., Riek-Loher, D., Bohrmann, B., Döbeli, H., Schubert, D., and Riek, R. (2005) 3D structure of Alzheimer's amyloid-β(1−42) fibrils. *Proc. Natl. Acad. Sci. U.S.A. 102*, 17342−17347.
(50) Nelson, R., Sawaya, M. R., Balbirnie, M., Madsen, A. Ø., Riekel, C., Grothe, R., and Eisenberg, D. (2005) Structure of the cross-β spine of amyloid-like fibrils. *Nature 435*, 773−778.
(51) Carrera, F., Marcos, E. S., Merkling, P. J., Chaboy, J. S., and Muñoz-Páez, A. (2004) Nature of metal binding sites in Cu(II) complexes with histidine and related N-coordinating ligands, as studied by EXAFS. *Inorg. Chem. 43*, 6674−6683.
(52) Parthasarathy, S., Long, F., Miller, Y., Xiao, Y., McElheny, D., Thurber, K., Ma, B., Nussinov, R., and Ishii, Y. (2011) Molecular-level examination of Cu^{2+} binding structure for amyloid fibrils of 40-residue Alzheimer's β by solid-state NMR spectroscopy. *J. Am. Chem. Soc. 133*, 3390−3400.
(53) Pedersen, J. T., Teilum, K., Heegaard, N. H., Østergaard, J., Adolph, H. W., and Hemmingsen, L. (2011) Rapid formation of a

preoligomeric peptide−metal−peptide complex following copper(II) binding to amyloid-β peptides. *Angew. Chem., Int. Ed. 50*, 2532−2535.
(54) Shearer, J., Callan, P. E., Tran, T., and Szalai, V. A. (2010) Cu K-edge X-ray absorption spectroscopy reveals differential copper coordination within amyloid-β oligomers compared to amyloid-β monomer. *Chem. Commun. 46*, 9137−9139.
(55) Marjanska, M., Curran, G. L., Wengenack, T. M., Henry, P.-G., Bliss, R. L., Poduslo, J. F., Jack, C. R., Jr., Uğurbil, K., and Garwood, M. (2005) Monitoring disease progression in transgenic mouse models of Alzheimer's disease with proton magnetic resonance spectroscopy. *Proc. Natl. Acad. Sci. U.S.A. 102*, 11906−11910.
(56) Shankar, G. M., Li, S., Mehta, T. H., Garcia-Munoz, A., Shepardson, N. E., Smith, I., Brett, F. M., Farrel, M. A., Rowan, M. J., Lemere, C. A., Regan, C. M., Walsh, D. M., Sabatini, B. L., and Selkoe, D. J. (2008) Amyloid-β protein dimers isolated directly from Alzheimer's brains impair synaptic plasticity and memory. *Nat. Med. 14*, 837−842.
(57) Kayed, B., Head, E., Thompson, J. L., McIntire, T. M., Milton, S. C., Cotman, C. W., and Glabe, C. G. (2003) Common structure of soluble amyloid oligomers implies common mechanism of pathogenesis. *Science 300*, 486−489.
(58) Gaggelli, E., Kozlowski, H., Valensin, D., and Valensin, G. (2006) Copper homeostasis and neurodegenerative disorders. *Chem. Rev. 106*, 1995−2044.
(59) Squitti, R., Ventriglia, M., Barbati, G., Cassetta, E., Ferreri, F., Forno, G. D., Ramires, S., Zappasodi, F., and Rossini, P. M. (2007) 'Free' copper in serum of Alzheimer's disease patients correlates with markers of liver function. *J. Neural Transm. 114*, 1589−1594.
(60) Barnham, K. J., Masters, C. L., and Bush, A. I. (2004) Neurodegenerative disease and oxidative stress. *Nat. Rev. Drug Discovery 3*, 205−214.
(61) Harris, E. D. (2000) Cellular copper transport and metabolism. *Annu. Rev. Nutr. 20*, 291−310.
(62) Kim, B.-E., Nevitt, T., and Thiele, D. J. (2006) Mechanisms for copper acquisition, distribution and regulation. *Nat. Chem. Biol. 4*, 176−185.
(63) Clarke, C. S., and Bannon, F. J. (2005) Serum albumin in Down syndrome with and without Alzheimer's disease. *Ir. J. Med. Sci. 174*, 4−8.
(64) Koistinaho, M., and Koistinaho, J. (2005) Interactions between Alzheimer's disease and cerebral ischemia: Focus on inflammation. *Brain Res. Rev. 48*, 240−250.
(65) Little, J. R., Cook, A., Cook, S. A., and Maclntyre, W. J. (1981) Microcirculatory obstruction in focal cerebral ischemia: Albumin and erythrocyte transit. *Stroke 12*, 218−223.
(66) Sbarouni, E., Georgiadou, P., and Voudris, V. (2011) Ischemia modification albumin changes: Review and clinical implications. *Clin. Chem. Lab. Med. 49*, 177−184.
(67) Boada, M., Ortiz, P., Anaya, F., Hernández, I., Muñoz, J., Núñez, L., Olazarán, J., Roca, I., Cuberas, G., Tárraga, L., Buendia, M., Pla, R. P., Ferre, I., and Páez, A. (2009) Amyloid-targeted therapeutics in Alzheimer's disease: Use of human albumin in plasma exchange as a novel approach for Aβ mobilization. *Drug News Perspect. 22*, 325−339.